THE JOURNAL OF PHYSICAL CHEMISTRY B

Article

pubs.acs.org/JPCB

Effect of Compressive Force on Unbinding Specific Protein−Ligand Complexes with Force Spectroscopy

Carleen M. Bowers,[†,§] David A. Carlson,[†,§] Monica Rivera,[‡] Robert L. Clark,*[,‡] and Eric J. Toone*[,†]

[†]Department of Chemistry, Duke University, Durham, North Carolina 27708, United States

[‡]Hajim School of Engineering and Applied Sciences, University of Rochester, Rochester, New York 14627, United States

Supporting Information

ABSTRACT: Atomic force microscopy (AFM) is used extensively for the investigation of noncovalent molecular association. Although the technique is used to derive various types of information, in almost all instances the frequency of complex formation, the magnitude of rupture forces, and the shape of the force−distance curve are used to determine the behavior of the system. We have used AFM to consider the effect of contact force on the unbinding profiles of lactose−galectin-3, as well as the control pairs lactose−KDPG aldolase, and mannose−galectin-3, where the interacting species show negligible solution-phase affinity. Increased contact forces (>250 pN) resulted in increased probabilitites of binding and decreased blocking efficiencies for the cognate ligand−receptor pair lactose−G3. Increased contact force applied to two control systems with no known affinity, mannose−G3 and lactose−KDPG aldolase, resulted in nonspecific ruptures that were indistinguishable from those of specific lactose−G3 interactions. These results demonstrate that careful experimental design is vital to the production of interpretable data, and suggest that contact force minimization is an effective technique for probing the unbinding forces and rupture lengths of only specific ligand−receptor interactions.

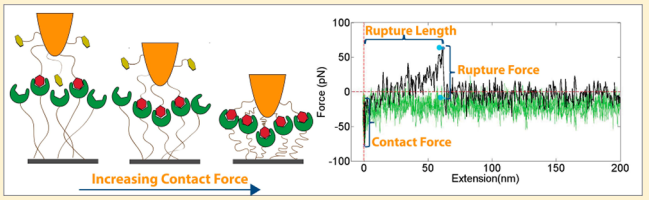

INTRODUCTION

Noncovalent associative forces in aqueous milieu control myriad biological processes and are the basis for many biosensing technologies.[1−4] Because of its ability to spatially manipulate and measure forces between individual molecules, the atomic force microscope (AFM) is well suited for the consideration of noncovalent interactions.[5−7] Noncovalent rupture forces between biotin and avidin,[8,9] complementary DNA strands,[10−14] antibody−antigen,[15,16] and protein−carbohydrate[17−19] complexes have been studied using AFM-based methods.

Molecular recognition force microscopy (MRFM) has been widely applied to the study of protein unfolding and biomolecular association, in both aqueous and nonaqueous environments.[20,21] Although the goal of MRFM is to study specific biomolecular interactions, the shape of unbinding profiles, the probability of binding during an approach−retract cycle, and degree of nonspecific adhesion are highly dependent on a set of experimental variables including, but not limited to, the specific biomolecules used,[8−10,15,17,18] the nature and geometry of immobilization,[22] and composition of the solution in which molecular interactions take place.[23,24]

An important goal of our research is to develop AFM methodologies that facilitate evaluation of thermodynamic parameters by characterizing specific noncovalent interactions between individual immobilized molecules.[18,25] Recently, we reported an AFM sensing technique using the carbohydrate binding protein galectin-3 (G3) and tip-immobilized lactose. A binding constant for the immobilized lactose−G3 complex was determined from the variation of binary probability bound complex formation as a function of soluble ligand.[18] The formation of nonspecific complexes, however, can complicate force curve analysis, obfuscating the true fractional probability of specific complex formation. This differentiation is not straightforward: the forces required to rupture noncovalent interactions are weak (on the order of 10^1−10^2 pN)[26] but of similar magnitude to specific noncovalent forces, and, operative over the same length scales as specific interactions. Clearly, the effective interpretation of data from molecular recognition force spectroscopy relies exquisitely on experimental protocols that both minimize the formation of nonspecific complexes and effectively discriminate between specific and nonspecific complexes.

In a typical MRFM experiment, the sample is driven toward the tip until a predetermined contact force (piconewton to nanonewton scale) is achieved. Although achieving physical proximity of receptor and ligand is obviously essential to facilitate binding, excessive force between immobilized species confounds data interpretation. Specifically, compressive strain has been reported to cause protein denaturation[27,28] and tip fouling.[29] Efforts have been made to avoid the complications resulting from sample degradation through the use of "compression-free" force spectroscopy, in which close proximity is achieved without tip−sample contact.[30] To date,

Received: September 21, 2012
Revised: March 14, 2013
Published: March 28, 2013

however, no systematic study of the effect of compressive force on binding probability, blocking efficiency, rupture force, and rupture length has been conducted.

Here we investigate the effect of applied contact force on the probability of observing a rupture event, the normalized number of blockable rupture events per pull, and rupture force and length distribution in force versus extension plots. The cognate ligand−receptor pair lactose−G3 along with two control systems with no known affinity, mannose−G3 and lactose-2-keto-3-deoxy-6-phosphogluconate (KDPG) aldolase, were studied.

EXPERIMENTAL METHODS

Syntheses of NTA−maleimide linker **1**, mercaptopentyl lactose (**2**), and mercaptopentyl mannose (**3**) are described in the Supporting Information.

Expression and Purification of Murine His_6-Tagged Galectin-3. The his_6-tagged galectin-3 was expressed and purified as described by Snyder et al.[18] The gene for wild-type galectin-3 was obtained by PCR amplification from the plasmid prCBP35s (obtained from Dr. J. L. Wang) and digested with *Eco*RI and *Bam*HI. The digested PCR product was ligated into a similarly prepared pET28b plasmid and transformed into BL21 (DE3) cells. A 5 mL portion of TB/Kanamycin (30 μg/mL) was inoculated with a single colony of BL21 (DE3) cells and incubated at 37 °C overnight. Cells were grown until the optical density at 600 nm (OD_{600}) reached 0.6−0.8 and expression was induced during 3 h with 125 mg L^{-1} isopropyl thiogalactopyranoside (IPTG). Cells were harvested by centrifugation and lysed by sonication, and the supernatant was applied to 10 mL of His Bind resin (Novagen, San Diego, CA). Galectin-3 was isolated according to manufacturer's instructions and dialyzed against EDTA (1 mM) in sodium phosphate (50 mM, pH 7.5) for 8 h, followed by dialysis against sodium phosphate (50 mM, pH 7.5) for 24 h to remove imidazole and EDTA.

Expression and Purification of His_6-Tagged 2-Keto-3-deoxy-6-phosphogluconate (KDPG) Aldolase. A plasmid containing the gene KDPG-pet36, which encodes his_6-tagged KDPG aldolase, was transformed into BL21 CodonPlus (DE3)-RIL cells. The transformation mixture was plated onto an LB/Kan (50 mg mL^{-1}) plate and incubated overnight at 37 °C. A single colony from the LB/Kan plate was introduced into 50 mL of TB/Kan (50 mg mL^{-1}). The culture was incubated at 37 °C for 16 h and then 10 mL was transferred to 1 L of TB/Kan (50 mg mL^{-1}) and shaken at 37 °C until an OD_{600} of 0.8 was reached. Expression was induced by the addition of IPTG (230 mg L^{-1}, to 1 mM) to the cell culture. The induced culture was shaken at 37 °C for an additional 4 h. The cells were collected by centrifugation and lysed by sonication, and the supernatant was applied to 10 mL of His Bind resin (Novagen, San Diego, CA). KDPG aldolase was isolated according to manufacturer's instructions and dialyzed into HEPES buffer (20 mM, pH 7.5) at 4 °C.[31]

Functionalization of Silicon Nitride AFM Tips. AFM tips (NP, Bruker, nominal spring constant of 0.120 N/nm) were rinsed thoroughly in methanol and water, dried under nitrogen, and cleaned in a plasma oxidizer (5 min, 100 W). Vapor-phase aminosilanization was accomplished using a protocol similar to that published by Riener et al.[32] Tips were placed in 50 mL glass bottles containing 2 mL vials of freshly distilled APTMS (30 μL) and triethylamine (10 μL) under an atmosphere of argon. After 2 h of incubation, the APTMS and triethylamine were removed. The bottle was flushed with argon and sealed for 2 days. Aminofunctionalized tips were rinsed with dichloromethane and immersed in a solution of NHS-PEG_{12}-Mal (Quanta BioDesign, 2 mM in dichloromethane) with pyridine (1% w/v) for 1 h, rinsed with ethanol and water, and dried under argon. The cantilevers were next submerged in an aqueous solution of mercaptopentyl lactoside (**2**) or mercaptopentyl mannoside (**3**) (2.25 mM) for 4 h at 37 °C, rinsed with water, and dried under argon.[18]

Functionalization of Silicon Samples. His_6-tagged galectin-3 was chelated to the surface using a protocol similar to that of Schmid et al.[33] Silicon wafers (prime grade ⟨100⟩, Silicon Quest Int.) were rinsed with methanol and water and dried under nitrogen. The surfaces were immediately placed in a plasma oxidizer (5 min, 100 W) in order to generate surface hydroxyl groups on the native SiO_2 layer. Oxidized surfaces were silanized with mercaptopropyltrimethoxysilane (MPTMS) using the procedure described for aminosilanization of AFM tips. This process generated reactive thiols on the surface that were subsequently reacted during 1 h with 0.2 mg mL^{-1} nitrilotriacetate (NTA)−maleimide linker **1** in sodium phosphate buffer (10 mM, pH 7.0). The surfaces were rinsed with water and then incubated for 5 min in $NiSO_4$ (50 mM). The surfaces were rinsed with water and bind buffer (50 mM imidazole, 20 mM Tris HCl, 0.5 M NaCl, pH 7.9) and then submerged in a solution of his_6-galectin-3 (50 μM) in sodium phosphate buffer (50 mM, pH 7.5) or his_6-KDPG aldolase (50 μM) in HEPES buffer (20 mM, pH 7.5) for 1 h, then immediately rinsed with bind buffer followed by PBS (pH 7.4).

Unbinding Experiments. Automated pulling experiments were carried out on a custom-built 3-axis AFM composed of a MultiMode head (Digital Instruments, Santa Barbara, CA) mounted on an *xy*- and *z*-positioning stages (Physik Instrumente, Auburn, MA).[34] For each experiment, 250 force curves were generated using an automated data collection routine.[34] The sample surface was brought into contact with the tip, held for a dwell time of 1 s, and then retracted at a constant velocity of 200 nm s^{-1}. The force loading rate (383 ± 183 pN/s) was determined from the slope on the force curve before an unbinding event; see Supporting Information. For contact force minimization experiments, software parameters were optimized to achieve contact forces (<100 pN) for each pull. Following data collection, the photodetector was calibrated, and a cantilever spring constant was determined using the thermal noise method.[35] The photodetector was calibrated prior to data collection for force trigger experiments. The sample was then driven toward the tip until a desired contact force was achieved (250 or 1000 pN). Unblocked experiments were carried out in the presence of PBS, pH 7.4. Blocking experiments were a carried out in the presence β-methyl lactose (10 mM in PBS, pH 7.4); at this concentration of ligand, 98% of available binding sites should be occupied by soluble lactose, assuming an immobilized binding constant of 6400 M^{-1}.[18]

RESULTS AND DISCUSSION

Immobilization of Lactose and Mannose on Silicon Nitride Tips. Aminofunctionalization of silicon nitride AFM tips was accomplished using the method of Ebner et al.[36] Briefly, plasma-cleaned tips were subject to vapor-phase deposition of 3-aminopropyltrimethoxysilane (APTMS). The resulting amine-terminated surface was conjugated to a heterobifunctional (oligoethylene)glycol linker (Mal-PEG_x-NHS ester, Quanta Biodesign). Poly(ethylene glycol) (PEG)

dx.doi.org/10.1021/jp309393s | J. Phys. Chem. B 2013, 117, 4755−4762

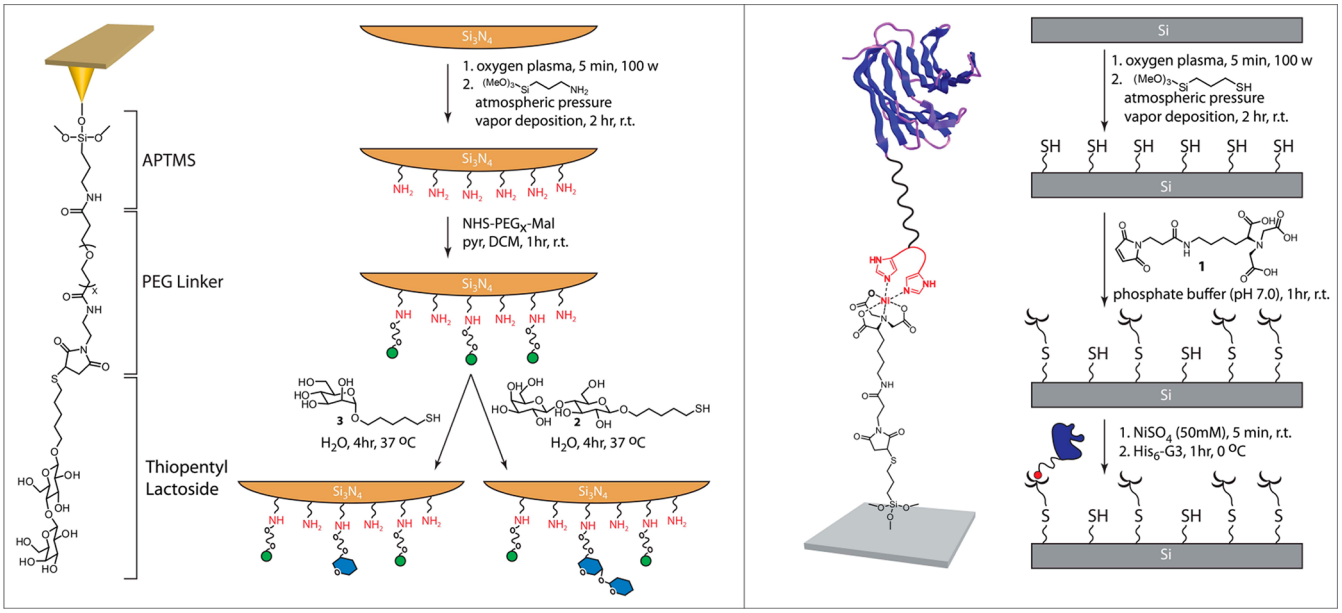

Figure 1. Molecular assemblies for pulling experiments. Thiopentyl lactoside (**2**) and thiopentyl mannoside (**3**) were conjugated to an aminosilanized silicon nitride tip through a bifunctional poly(ethylene glycol) linker (NHS-PEG$_{12}$Mal). His$_6$-galectin-3 and his$_6$-KDPG aldolase were immobilized via N-terminal-his$_6$-Ni^{2+} coordination to a covalently anchored NTA linker **1** on mercaptosilanized silicon ⟨111⟩. A crystal structure of the G3 C-terminal CRD is shown. The disordered N-terminal G3 CLR with his$_6$ tag is also represented (red line).

spacers have proven to be suitable cross-linkers for force spectroscopy.[37] Three different linkers lengths were initially investigated (x = 2, 6, and 12). The longer linker, Mal-PEG$_{12}$-NHS ester, provided additional flexibility and mobility and increased the total observed binding probability (see Supporting Information, Figure S2). Thiopentyl lactoside (**2**) and thiopentyl mannoside (**3**) were covalently bound to the surface by conjugate addition to the reactive maleimide functionality (Figure 1).[18] Thiopentyl mannoside, a molecule for which galectin-3 has no known affinity, was used as a negative control.

Immobilization of Galectin-3 and KDPG Aldolase. Vapor deposition of freshly distilled 3-mercaptopropyltrimethoxysilane (MPTMS) onto plasma-oxidized silicon ⟨111⟩ samples provided thiol-terminated surfaces. Conjugate addition of surface thiols to maleimide **1**[20] provided a chelation site for Ni^{2+}-mediated immobilization of his$_6$-G3 and his$_6$-KDPG aldolase via his$_6$-Ni^{2+}-NTA chelation. The terminal his$_6$ tag, routinely used for affinity purification of galectin-3 and KDPG aldolase, does not significantly affect solution-phase affinities of either biomolecule.[38]

Figure 1 describes the molecular assemblies used for this investigation. The surface-immobilized carbohydrate binding protein, galectin-3, binds immobilized lactose with an affinity of ~6400 M^{-1},[18] and displays no significant affinity for mannose. At the C-terminus, a 137 amino acid carbohydrate recognition domain (CRD) is oriented away from the surface and a disordered N-terminal 120 amino acid collagen-like-repeat (CLR) is anchored by an N-terminal his$_6$ tag. Chelation-based immobilization of proteins has previously been utilized to anchor other his$_6$ tagged proteins to NTA-terminated monolayers for AFM binding studies.[7,39,40] In crystalline form the G3 CRD is ~4.5 nm across its longest axis; in fully extended form, the CLR is ~44 nm in length. The total estimated tip to surface length of immobilized lactose bound to a properly folded CRD with fully extended CLR and linkers is approximately 60 nm.

Hexa-histidine tagged KDPG aldolase, a protein with no measurable affinity for hemiacetal forms of glucose, galactose, or lactose, was used as a negative control. KDPG aldolase binds the open chain form of 2-keto-3-deoxy-6-phosphogluconate and related straight-chain aldehydes.[41] Active KDPG aldolase exists in solution as a trimeric assembly of identical subunits 3.9 nm in length.[42] The total estimated length, from tip to sample, of the KDPG aldolase construct is 16.4 nm. Because of its decreased molecular length and lack of affinity for lactose, no specific interactions between KDPG aldolase and tip-immobilized lactose were expected.

Data Collection Routines. Our goal was to gain insight into the effect of compressive forces on the data produced during molecular recognition force microscopy experiments. We evaluated complex formation using three pulling routines: a custom force minimization routine (F_{min}), which can be optimized to reliably achieve sub-100 pN contact forces[34] (Figure 2), and force trigger routines with nominal contact

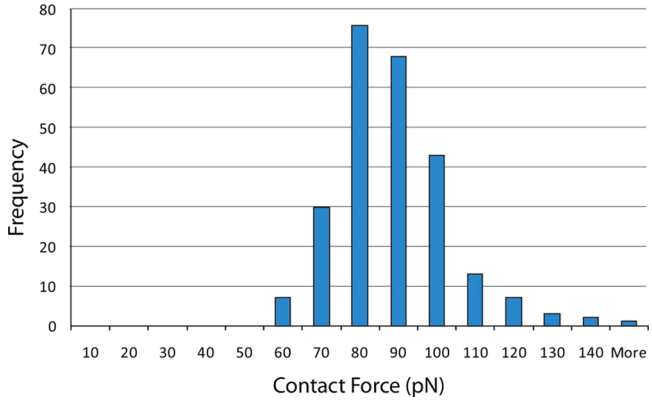

Figure 2. Histogram of observed contact forces (F_c) for the lactose–G3 system using the Fmin data collection routine to complete 250 approach–retraction cycles.

dx.doi.org/10.1021/jp309393s | J. Phys. Chem. B 2013, 117, 4755–4762

force (F_{cnom}) triggers of 250 or 1000 pN at a rate of 200 nm s^{-1}. Minimal contact forces were achieved by using a custom-built threshold-based F_{min} pulling routine for lactose−G3, lactose−KDPG aldolase, and mannose−G3 systems. The custom pulling routine uses data recorded during the first approach−retract cycle to alter the position of the sample surface so that minimal contact force (<100 pN) is exerted on the tip throughout the next approach−retract cycle while achieving tip−sample proximity. All threshold values and adjustments were optimized using a previously reported automated pulling protocol.[34] To achieve higher contact forces, a force trigger routine was utilized. The sample was driven to toward the surface until a nominal contact force (F_{cnom} = 250 or 1000 pN) was reached.

Data Analysis. Force versus extension plots were analyzed according to a predefined set of rules and applied uniformly across all data sets. The force curves generated during approach−retract cycles provided rupture forces and lengths for each bound interaction. The overall magnitude of tip deflection was defined as the vertical difference between the apex and the midpoint of the noise at the base of each rupture event. The intensity and vertical position signals were low-pass filtered by a dual 24 dB octave filter to remove noise. Rupture length was defined as the molecular extension at the apex of the unbinding event.

Nonspecific interactions or adhesion arise from other attractive forces for which no true binding equilibrium expression can be written. Specifically, the introduction of soluble ligand does not drive the system toward the unbound state. Removal of the collagen-like repeat (CLR) domain has no effect on the binding behavior of the G3 carbohydrate recognition domain,[38] and we assume that lactose−G3 affinity is not affected by extension of the CLR. Unbinding beyond the length of the fully unfolded system implies compression-induced processes that extend the overall length of the interacting system. It is conceivable that high F_c results in a "snow plow" effect as the cantilever tip is driven into and rasters across the surface. A possible result from this process is ablation of protein from the surface and tip fouling, through transfer of protein aggregates from sample to tip. As the AFM probe is pushed onto the surface, there is a possibility that material is being physically adsorbed to the probe affecting the length of the system.[30] It was also assumed that specific lactose−G3 binding is not possible if the CRD is denatured or partially unfolded.[28]

Probability of Observing a Rupture and Blocking Efficiency. Of the three systems studied here, only lactose−G3 forms a specific complex. A fundamental assumption is that the binding sites of immobilized G3 can be occupied by soluble ligand thereby preventing the formation of specific bound interactions with lactose-modified tips, an assumption supported by previous studies.[18] We therefore anticipated that the addition of soluble β-methyl lactose would diminish the probability of observing specific rupture events for this system. Additionally, all unbinding events observed after saturation of immobilized G3 with β-methyl lactose were interpreted as nonspecific adhesion.

Because there should be no affinity between mannose−G3 or lactose−KDPG aldolase, no specific bound interactions were expected for either of these systems. Furthermore, the addition of soluble β-methyl lactose should have no effect on the probability of observing a rupture for these systems.

As evident from Figure 3A, the probability of observing a rupture (ρ_{bind} = number of rupture-containing pulls/total pulls)

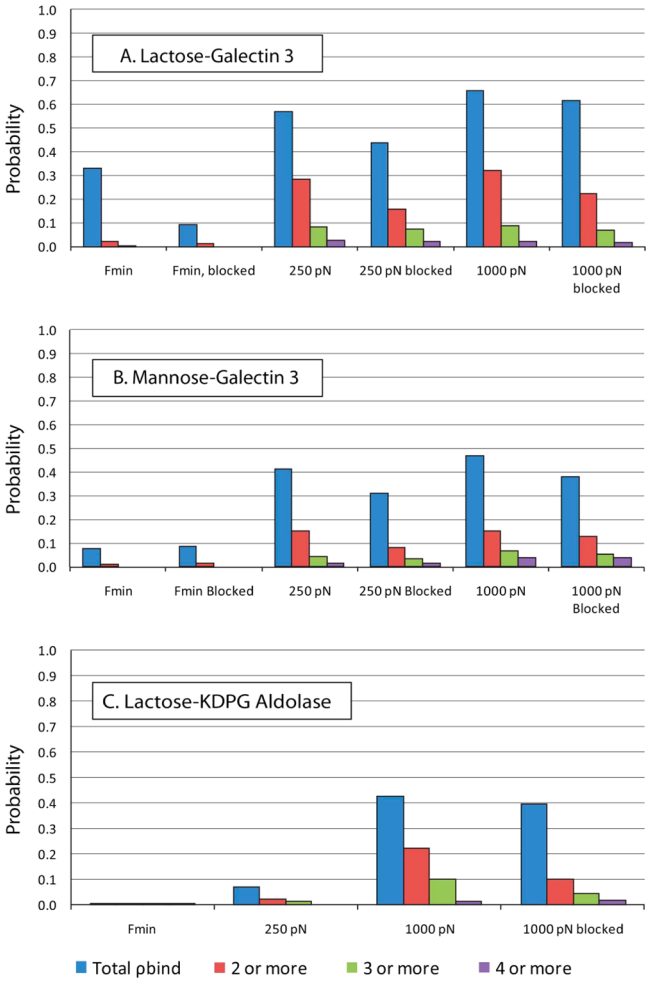

Figure 3. Probability of observing an unbinding event for the (A) lactose−G3, (B) mannose−G3, and (C) lactose−KDPG aldolase systems generated by F_{min}, force trigger (F_{cnom} = 250 pN), and force trigger (F_{cnom} = 1000 pN) pulling routines. The overall probability of observing an unbinding event (blue) for lactose−G3 increases with increasing contact force. The probability of observing two or more (red), three or more (green), and four or more events (violet) also increase with increasing contact force. The probability of observing an unbinding event for mannose−G3 and lactose−KDPG aldolase also increases with increasing contact force. All blocked experiments contained 10 mM soluble β-methyl lactose.

increased with increasing F_c, as did the number of rupture events per pull for the lactose−G3 system. Under the minimal compressive forces applied in the F_{min} routine, single rupture events predominated with ρ_{bind} of 0.33 and $\rho_{multiple}$ of 0.02. After blocking with β-methyl lactose (10 mM in PBS pH 7.4), ρ_{bind} decreased to 0.09, a 73% blocking efficiency. Based on immobilized lactose−G3 affinity,[18] 98% of surface sites should be blocked by soluble lactose.

Use of the force trigger protocol to apply significant contact forces (F_{cnom} = 250 pN) resulted in an increase in both the total probability of binding (ρ_{bind} = 0.57) and the probability of observing two or more ruptures ($\rho_{multiple}$ = 0.28) for the unblocked configuration. This probability was diminished to ρ_{bind} = 0.44 upon blocking with β-methyl lactose (10 mM in PBS pH 7.4), a 23% blocking efficiency.

dx.doi.org/10.1021/jp309393s | J. Phys. Chem. B 2013, 117, 4755−4762

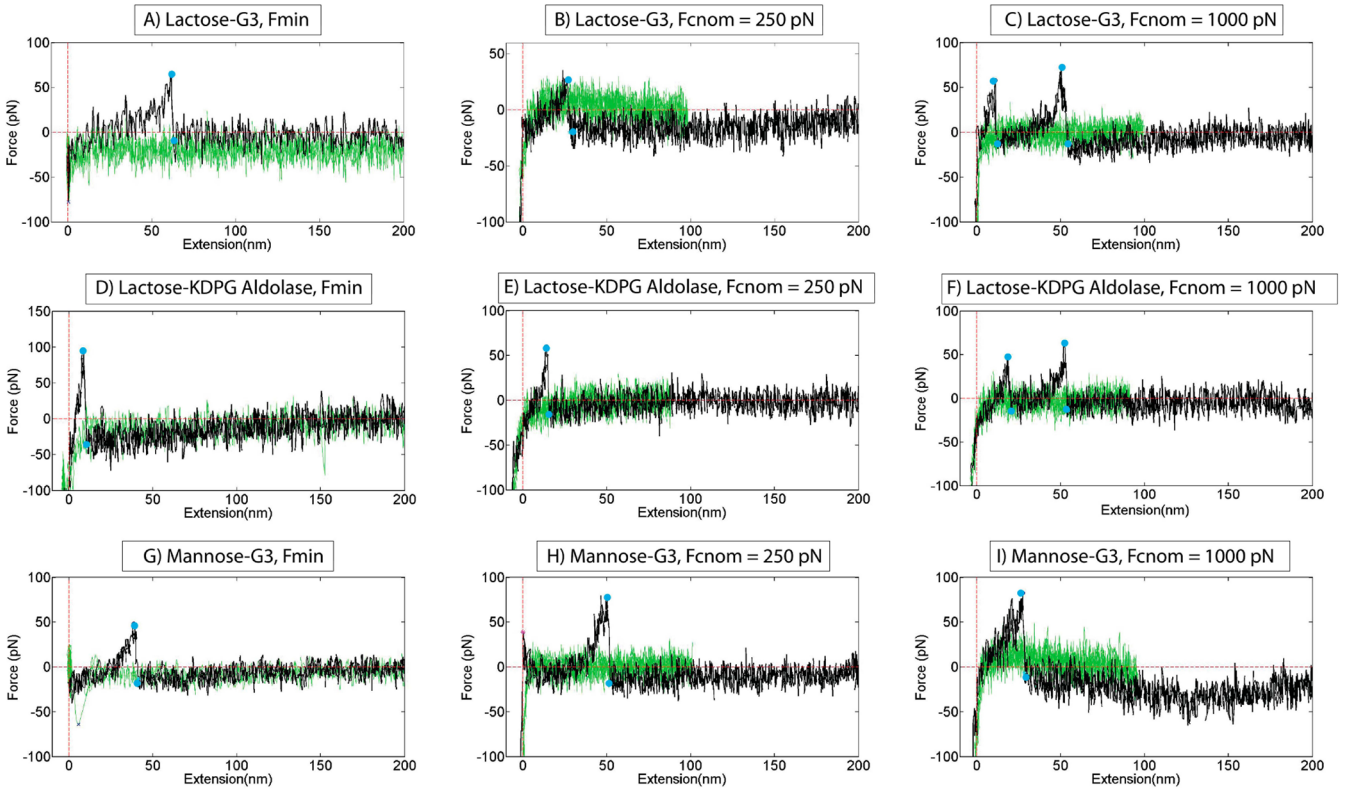

Figure 4. Representative force distance curves for the lactose−G3, lactose−KDPG aldolase, and mannose−G3 systems generated by F_{min}, force trigger (F_{cnom} = 250 pN), and force trigger (F_c = 1000 pN) pulling routines. Approach curves (green) and retraction curves (black) with unbinding events (blue circles) are depicted.

Under the maximum compressive force used for this study (F_{cnom} = 1000 pN), a significant increase in both probability of binding (ρ_{bind} = 0.66) and the number of multiple ruptures was observed for the unblocked system. This probability was diminished to ρ_{bind} = 0.62 upon blocking with β-methyl lactose (10 mM in PBS pH 7.4), a 6% blocking efficiency. Because we assume that all unbinding events observed after saturation of immobilized G3 with β-methyl lactose were nonspecific in nature, we conclude that nonspecific binding was responsible for approximately 94% of all unbinding events observed in the unblocked experiment.

In order to further investigate the effect of compressive forces on the integrity of the lactose-modified tip, a freshly prepared tip and sample were subjected to 50 approach−retract cycles using a force trigger of 1000 pN. The tip was then moved several micrometers laterally, and the F_{min} pulling protocol was utilized to generate 250 force curves. This probability of binding, ρ_{bind} = 0.09, was significantly lower than those measured in a typical F_{min} experiment (ρ_{bind} = 0.33). The repeated application of compressive forces on the order of 1000 pN possibly degrades the tip-immobilized lactose, rendering it unable to form specific complexes with G3.[28] It is also possible that high contact forces compromise the integrity of the hexahistidine−NTA complex at the surface.[40]

To better understand the effect of compressive force on the formation of nonspecific complexes, we repeated the entire protocol, but replaced thiopentyl lactoside (**2**) with thiopentyl mannoside (**3**), a ligand for which G3 has no known affinity. As evident from Figure 3B, few bound interactions were observed for both unblocked and blocked F_{min} experiments (ρ_{bind} = 0.08) and ($\rho_{multiple}$ = 0.01). Under compressive forces of 250pN ρ_{bind} increased to 0.41 and $\rho_{multiple}$ increased to 0.15. This probability was diminished to ρ_{bind} = 0.31 during blocking with β-methyl lactose (10 mM in PBS pH 7.4), representing a 24% blocking efficiency. Under compressive forces of 1000 pN, ρ_{bind} increased to 0.47 and $\rho_{multiple}$ remained 0.15. The overall probability was diminished by roughly 20% to ρ_{bind} = 0.38 upon blocking with β-methyl lactose (10 mM in PBS pH 7.4), a 19% blocking efficiency. The number of bound interactions per pull also increased with increasing compressive force. Given the lack of affinity of G3 for mannose, we attribute all observed interactions in configurations using mannose ligands to nonspecific events.

Similar trends were observed for the second control system, lactose−KDPG aldolase (Figure 3C). As expected, virtually no bound interactions (ρ_{bind} = 0.004) were observed using the F_c min protocol. On the other hand, ρ_{bind} increased to 0.07 and 0.42 using force triggers of F_{cnom} = 250 and 1000 pN, respectively. The probability using a force trigger of F_{cnom} = 1000 pN was not significantly diminished (ρ_{bind} = 0.40) upon blocking with β-methyl lactose (10 mM in PBS pH 7.4), a 5% blocking efficiency. The number of bound interactions per pull also increased. Given the lack of affinity of KDPG aldolase for lactose, we attribute all observed interactions to nonspecific processes.

Morphology of Force versus Extension Plots. A major goal of molecular recognition force microscopy is to obtain detailed information about the nature of the interacting molecular systems from force curve morphologies, particularly in the identification, isolation, and structural analysis of numerous ligand−receptor complexes.[6,7,43,44] In order to gain insight into how contact forces affect force−extension curves,

dx.doi.org/10.1021/jp309393s | J. Phys. Chem. B 2013, 117, 4755−4762

we carried out a systematic study using the three data collection routines previously described (F_{min} and force triggers F_{cnom} = 250 pN and F_{cnom} = 1000 pN) to probe the effect of compressive force on the morphology of force curves generated using the cognate binding system lactose−G3 and negative control molecular systems comprising lactose−KDPG aldolase and mannose−G3.

Figure 4 depicts typical force versus extension plots displaying rupture events for the lactose−G3, lactose−KDPG aldolase, and mannose−G3 systems. Evidence of binding can be seen in all retraction curves (black line).

Force signatures generated with the lactose−G3 system using F_{min} were generally similar in morphology to those shown in Figure 4A. As described previously, single rupture events predominated, with ∼73% of all observed ruptures attributed to specific binding and can be described by an equilibrium expression. Although we concluded in the previous section that nonspecific binding was present in ∼77% and ∼94% of all force curves that contained evidence of unbinding events using F_{cnom} = 250 and 1000 pN, respectively, the majority (>50%) of these force curves are indistinguishable from those generated using the F_{min} protocol (Figure 4, B and C). These results suggest that force curve morphology alone is insufficient to distinguish specific from nonspecific rupture events.

No specific bound complexes should arise during lactose−KDPG aldolase interaction. In the event, however, several force signatures for this system showed curves with morphologies similar or identical to those for specific lactose−G3 interactions. Although ruptures at short extensions (>10 nm) were frequently observed when utilizing the F_{min} and F_{cnom} = 250 pN pulling routines (Figure 4, D and E), higher compressive forces (F_{cnom} = 1000 pN) produced force curves identical to those of lactose−G3 (Figure 4F). Additionally several (presumably) nonspecific mannose−G3 rupture events showed curve shapes identical to those arising from specific lactose−G3 force signatures (Figure 4, G, H, and I). These results further suggest that force curve morphology alone is insufficient to determine the specific nature of a rupture. Thus, the mere presence of an unbinding event in the force curve does not implicitly arise from the rupture of a specific bound interaction but may instead arise from nonspecific adhesion.

Rupture Force Distributions. The distribution of rupture forces for the lactose−G3 system is unimodal with the most probable rupture force equal to 60 ± 28 pN for all applied contact forces (Figure 5A), in good agreement with previously reported forces of 50 ± 10 pN using the same system at equivalent retraction rates.[18] This rupture force value is typical for carbohydrate−lectin interactions and in agreement with previously reported values at similar loading rates, suggesting the interaction between lactose and G3 involves binding in the carbohydrate binding site.[17,45] The histogram profiles of Figure 5A are similar regardless of applied F_c in all respects except frequency. Thus, rupture force histogram profile alone is not indicative of specific binding. If conclusions concerning the specificity of the interacting species were made from the rupture force histogram alone, we would assume no difference between data collected using F_{min} and the force trigger (F_{cnom} = 1000) other than ρ_{bind}. However, there is clearly a difference in blocking efficiency and therefore the occurrence of specific interactions (Figure 5A). Thus, blocking experiments are essential for determining the specificity of the observed molecular interactions.

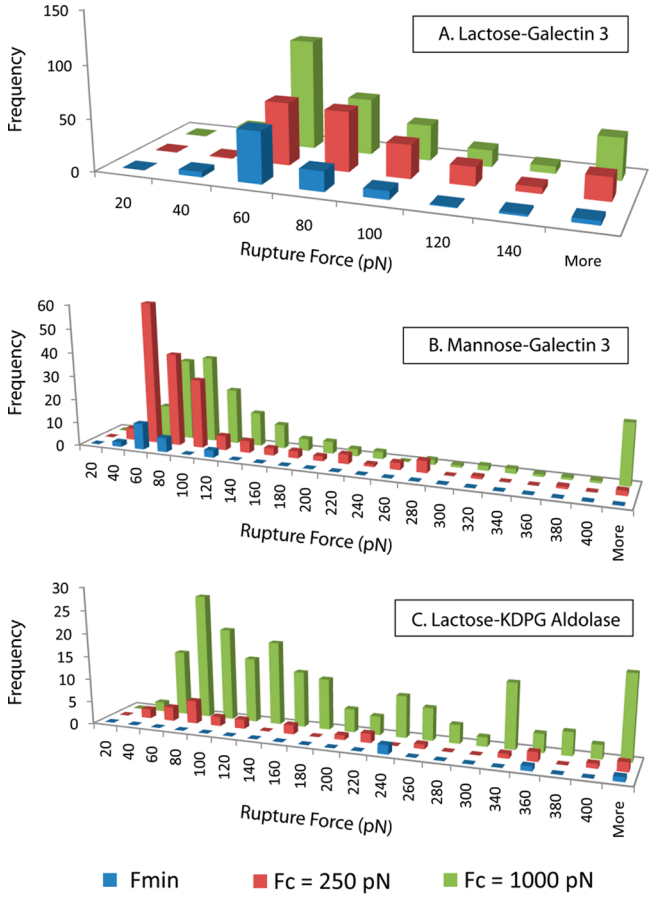

Figure 5. Histogram of rupture forces observed for (A) lactose−G3, (B) mannose−G3, and (C) lactose−KDPG aldolase using force minimization (blue), and force triggers of 250 pN (red) and 1000 pN (green).

In contrast to the lactose−G3 system, the presumably nonspecific interactions between mannose and G3 and between lactose and KDPGal aldolase produced a broader distribution of rupture forces (Figure 5B,C). The frequency of larger rupture forces increases significantly with increasing F_c.

Rupture Length Distributions. The total extended length of a lactose−G3 molecular system containing a folded and functional CRD is approximately 60 nm (Figure 1). Removal of the collagen-like repeat (CLR) using collagenase has no effect on the binding behavior of the carbohydrate recognition domain, and we thus assume that specific lactose−G3 affinity is unaffected by the extension of the CLR. We also assume that specific lactose−G3 affinity is not possible if the CRD is denatured or partially unfolded. Rupture lengths beyond 60 nm may indicate protein unfolding, assuming partially unfolded protein retains at least some affinity, or interfacial G3 aggregation. All ruptures at extensions less than 10 nm were considered nonspecific adhesion, e.g., surface−surface, linker−surface, or linker−linker interactions. The addition of soluble β-methyl lactose has no effect on observing nonspecific adhesion, the probability of observing these events was similar for unblocked (0.02) and blocked (0.05) lactose−G3 experiments using the F_{min} protocol.

A histogram of rupture lengths were plotted for all applied contact forces for the lactose−G3, mannose−G3, and lactose−KDPG aldolase systems (Figure 6). Under minimal contact forces the rupture length histogram profile for the lactose−G3

dx.doi.org/10.1021/jp309393s | J. Phys. Chem. B 2013, 117, 4755−4762

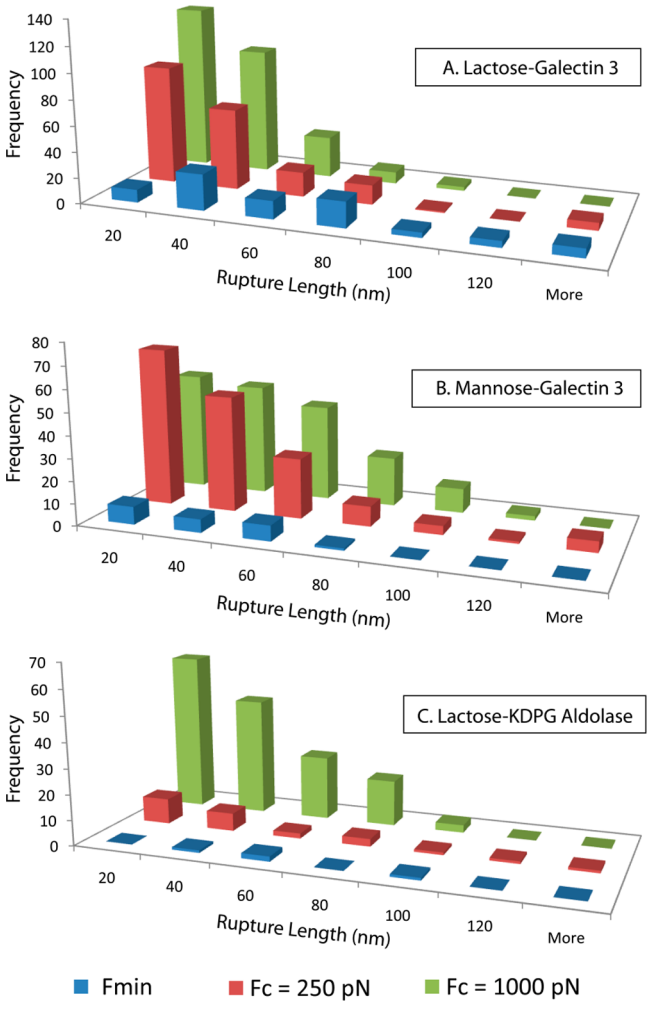

Figure 6. Histogram of rupture lengths observed for (A) lactose−G3, (B) mannose−G3, and (C) lactose−KDPG aldolase using force minimization (blue), and force triggers of 250 pN (red) and 1000 pN (green).

interaction is unimodal with a distribution centroid near 50 nm. The distribution of lengths around 80 nm could be associated with nonspecific, unblockable binding events. Shorter rupture length bins become more populated using force triggers of 250 and 1000 pN. Rupture length distributions for nonspecific mannose−G3 and lactose−KDPG aldolase interactions decrease in frequency at longer lengths. The rupture length distribution for lactose−KDPG aldolase is shifted to shorter lengths, presumably due to the shorter molecular length of the interacting system (16.4 nm) and the lack of an extendable collagen-like repeat.

The increase in rupture frequency is not necessarily related to an increase in specific binding events. Again, the biophysical significance of ruptures cannot be fully understood on the basis of rupture length histograms alone. Rather, blocking experiments remain essential for the interpretation of cantilever movement.

CONCLUSIONS

Our goal here was to interpret cantilever movement in terms of specific noncovalent interaction between immobilized biomolecules. We demonstrated that contact force dramatically affects molecular recognition force microscopy experiments. For cognate binding partners lactose and G3, minimal contact forces introduced minimal unblockable artifacts into data sets. Increased contact forces resulted in increased probabilities of binding concomitant with decreased blocking efficiencies, i.e., a greater number of unblockable artifacts resulting from greater contact forces. For molecular systems with no known affinity, mannose−G3 and lactose−KDPG aldolase, we demonstrated that increased contact forces resulted in nonspecific ruptures that were similar or identical in morphology, rupture force, and rupture length to those of specific lactose−G3 interactions. Thus, the biophysical significance of rupture events cannot be fully understood on the basis of force curve shape, rupture force distribution, or rupture length distribution alone. Blocking experiments remain essential for the interpretation of cantilever movement. Therefore, it is essential to design MRFM data collections routines that minimize contact forces to ensure that ruptures originate from specific, blockable interactions

ASSOCIATED CONTENT

Supporting Information

Experimental details; Figure S2, probability of observing a binding even between lactose−G3 as a function of linker length; Figure S3, histogram of rupture forces using different PEG linker lengths. This material is available free of charge via the Internet at http://pubs.acs.org.

AUTHOR INFORMATION

Corresponding Author

*E-mail: eric.toone@duke.edu.

Author Contributions

[§]These authors contributed equally.

Notes

The authors declare no competing financial interest.

ACKNOWLEDGMENTS

We thank Dr. Alexander Shestopalov for helpful discussions and Dr. Stephen Craig for allowing us to use his AFM.

REFERENCES

(1) Carlson, C. B.; Mowery, P.; Owen, R. M.; Dykhuizen, E. C.; Kiessling, L. L. Selective Tumor Cell Targeting using Low-Affinity, Multivalent Interactions. *ACS Chem. Biol.* **2007**, *2*, 119−127.

(2) Dimick, S. M.; Powell, S. C.; McMahon, S. A.; Moothoo, D. N.; Naismith, J. H.; Toone, E. J. On the Meaning of Affinity: Cluster Glycoside Effects and Concanavalin A. *J. Am. Chem. Soc.* **1999**, *121*, 10286−10296.

(3) Lundquist, J. J.; Toone, E. J. The Cluster Glycoside Effect. *Chem. Rev.* **2002**, *102*, 555−578.

(4) Mammen, M.; Choi, S. K.; Whitesides, G. M. Polyvalent Interactions in Biological Systems: Implications for Design and Use of Multivalent Ligands and Inhibitors. *Angew. Chem., Int. Ed.* **1998**, *37*, 2755−2794.

(5) Janshoff, A.; Steinem, C. Energy Landscapes of Ligand-Receptor Couples Probed by Dynamic Force Spectroscopy. *Chemphyschem* **2001**, *2*, 577−579.

(6) Bizzarri, A. R.; Cannistraro, S. Atomic Force Spectroscopy in Biological Complex Formation: Strategies and Perspectives. *J. Phys. Chem. B* **2009**, *113*, 16449−16464.

(7) Hinterdorfer, P.; Dufrene, Y. F. Detection and Localization of Single Molecular Recognition Events Using Atomic Force Microscopy. *Nat. Methods* **2006**, *3*, 347−355.

(8) Florin, E. L.; Moy, V. T.; Gaub, H. E. Adhesion Forces between Individual Ligand-Receptor Pairs. *Science* **1994**, *264*, 415−417.

(9) Moy, V. T.; Florin, E. L.; Gaub, H. E. Intermolecular Forces and Energies between Ligands and Receptors. *Science* **1994**, *266*, 257−259.
(10) Lee, G. U.; Chrisey, L. A.; Colton, R. J. Direct Measurement of the Forces between Complementary Strands of DNA. *Science* **1994**, *266*, 771−773.
(11) Albrecht, C.; Blank, K.; Lalic-Multhaler, M.; Hirler, S.; Mai, T.; Gilbert, I.; Schiffmann, S.; Bayer, T.; Clausen-Schaumann, H.; Gaub, H. E. DNA A Programmable Force Sensor. *Science* **2003**, *301*, 367−370.
(12) Nguyen, T. H.; Steinbock, L. J.; Butt, H. J.; Helm, M.; Berger, R. Measuring Single Small Molecule Binding via Rupture Forces of a Split Aptamer. *J. Am. Chem. Soc.* **2011**, *133*, 2025−2027.
(13) Serpe, M. J.; Rivera, M.; Kersey, F. R.; Clark, R. L.; Craig, S. L. Time and Distance Dependence of Reversible Polymer Bridging Followed by Single-Molecule Force Spectroscopy. *Langmuir* **2008**, *24*, 4738−4742.
(14) Serpe, M. J.; Whitehead, J. R.; Rivera, M.; Clark, R. L.; Craig, S. L. Single-Molecule Force Spectroscopy of DNA-Based Reversible Polymer Bridges: Surface Robustness and Homogeneity. *Colloids Surf., A* **2009**, *346*, 20−27.
(15) Hinterdorfer, P.; Baumgartner, W.; Gruber, H. J.; Schilcher, K.; Schindler, H. Detection and Localization of Individual Antibody-Antigen Recognition Events by Atomic Force Microscopy. *Proc. Natl. Acad. Sci. U.S.A.* **1996**, *93*, 3477−3481.
(16) Wagner, C.; Singer, D.; Ueberschar, O.; Stangner, T.; Gutsche, C.; Hoffmann, R.; Kremer, F. Dynamic Force Spectroscopy on the Binding of Monoclonal Antibodies and tau Peptides. *Soft Matter* **2011**, *7*, 4370−4378.
(17) Dettmann, W.; Grandbois, M.; Andre, S.; Benoit, M.; Wehle, A. K.; Kaltner, H.; Gabius, H. J.; Gaub, H. E. Differences in Zero-Force and Force-Driven Kinetics of Ligand Dissociation from Beta-Galactoside-Specific Proteins (Plant and Animal Lectins, Immunoglobulin G) Monitored by Plasmon Resonance and Dynamic Single Molecule Force Microscopy. *Arch. Biochem. Biophys.* **2000**, *383*, 157−170.
(18) Snyder, P. W.; Lee, G.; Marszalek, P. E.; Clark, R. L.; Toone, E. J. A Stochastic, Cantilever Approach to the Evaluation of Solution Phase Thermodynamic Quantities. *Proc. Natl. Acad. Sci. U.S.A.* **2007**, *104*, 2579−2584.
(19) Touhami, A.; Hoffmann, B.; Vasella, A.; Denis, F. A.; Dufrene, Y. F. Probing Specific Lectin-Carbohydrate Interactions Using Atomic Force Microscopy Imaging and Force Measurements. *Langmuir* **2003**, *19*, 1745−1751.
(20) Lee, G.; Abdi, K.; Jiang, Y.; Michaely, P.; Bennett, V.; Marszalek, P. E. Nanospring Behaviour of Ankyrin Repeats. *Nature* **2006**, *440*, 246−249.
(21) Yu, H.; Liu, X.; Neupane, K.; Gupta, A. N.; Brigley, A. M.; Solanki, A.; Sosova, I.; Woodside, M. T. Direct Observation of Multiple Misfolding Pathways in a Single Prion Protein Molecule. *Proc. Natl. Acad. Sci. U.S.A.* **2012**, *109*, 5283−5288.
(22) Brogan, K. L.; Schoenfisch, M. H. Influence of Antibody Immobilization Strategy on Molecular Recognition Force Microscopy Measurements. *Langmuir* **2005**, *21*, 3054−3060.
(23) Brogan, K. L.; Shin, J. H.; Schoenfisch, M. H. Influence of Surfactants and Antibody Immobilization Strategy on Reducing Nonspecific Protein Interactions for Molecular Recognition Force Microscopy. *Langmuir* **2004**, *20*, 9729−9735.
(24) Wakayama, J.; Sekiguchi, H.; Akanuma, S.; Ohtani, T.; Sugiyama, S. Methods for Reducing Nonspecific Interaction in Antibody-Antigen Assay via Atomic Force Microscopy. *Anal. Biochem.* **2008**, *380*, 51−58.
(25) Bowers, C. M.; Carlson, D. A.; Shestopalov, A. A.; Clark, R. L.; Toone, E. J. A General and Efficient Cantilever Functionalization Technique for AFM Molecular Recognition Studies. *Biopolymers* **2012**, *97*, 761−765.
(26) Grandbois, M.; Beyer, M.; Rief, M.; Clausen-Schaumann, H.; Gaub, H. E. How Strong is a Covalent Bond? *Science* **1999**, *283*, 1727−1730.
(27) Berry, M.; McMaster, T. J.; Corfield, A. P.; Miles, M. J. Exploring the Molecular Adhesion of Ocular Mucins. *Biomacromolecules* **2001**, *2*, 498−503.
(28) Kodama, T.; Ohtani, H.; Arakawa, H.; Ikai, A. Observation of the Destruction of Biomolecules under Compression Force. *Ultramicroscopy* **2005**, *105*, 189−195.
(29) Ikai, A.; Afrin, R.; Sekiguchi, H. Pulling and Pushing Protein Molecules by AFM. *Curr. Nanosci.* **2007**, *3*, 17−29.
(30) Sekiguchi, H.; Arakawa, H.; Okajima, T.; Ikai, A. Non-Destructive Force Measurement in Liquid using Atomic Force Microscope. *Appl. Surf. Sci.* **2002**, *188*, 489−492.
(31) Walters, M. J.; Toone, E. J. Pyruvate Aldolases in Chiral Carbon-Carbon Bond Formation. *Nat. Protoc.* **2007**, *2*, 1825−1830.
(32) Riener, C. K.; Stroh, C. M.; Ebner, A.; Klampfl, C.; Gall, A. A.; Romanin, C.; Lyubchenko, Y. L.; Hinterdorfer, P.; Gruber, H. J. Simple Test System for Single Molecule Recognition Force Microscopy. *Anal. Chim. Acta* **2003**, *479*, 59−75.
(33) Schmid, E. L.; Keller, T. A.; Dienes, Z.; Vogel, H. Reversible Oriented Surface Immobilization of Functional Proteins on Oxide Surfaces. *Anal. Chem.* **1997**, *69*, 1979−1985.
(34) Rivera, M.; Morris, C.; Carlson, D.; Toone, E. J.; Cole, D. G.; Clark, R. L. *Proc. ASME 2009 Int. Des. Eng. Tech. Conf. Comput. Inf. Eng. Conf.* **2009**, *6*, 731−736.
(35) Hutter, J. L.; Bechhoefer, J. Calibration of Atomic-Force Microscope Tips (Vol 64, Pg 1868, 1993). *Rev. Sci. Instrum.* **1993**, *64*, 3342−3342.
(36) Ebner, A.; Hinterdorfer, P.; Gruber, H. J. Comparison of Different Aminofunctionalization Strategies for Attachment of Single Antibodies to AFM Cantilevers. *Ultramicroscopy* **2007**, *107*, 922−927.
(37) Hinterdorfer, P. K., F.; Raab, A.; Gruber, H. J.; Baumgartner, W.; Kada, G.; Riener, C.; Wielert-Badt, S.; Borken, C.; Schindler, H. Poly(ethylene glycol): an Ideal Spacer for Molecular Recognition Force Microscopy/Spectroscopy. *Single Mol.* **2000**, *1*, 99−103.
(38) Luteran, A. E. Towards the Molecular Basis of Affinity in Monovalent and Multivalent Protein-Carbohydrate Interactions. Duke University, 2007.
(39) Schmitt, L.; Ludwig, M.; Gaub, H. E.; Tampe, R. A Metal-Chelating Microscopy Tip as a New Toolbox for Single-Molecule Experiments by Atomic Force Microscopy. *Biophys. J.* **2000**, *78*, 3275−3285.
(40) Verbelen, C.; Gruber, H. J.; Dufrene, Y. F. The NTA-HiS(6) Bond is Strong Enough for AFM Single-Molecular Recognition Studies. *J. Mol. Recognit.* **2007**, *20*, 490−494.
(41) Shelton, M. C.; Cotterill, I. C.; Novak, S. T. A.; Poonawala, R. M.; Sudarshan, S.; Toone, E. J. 2-keto-3-deoxy-6-phosphogluconate aldolases as Catalysts for Stereocontrolled Carbon-Carbon Bond Formation. *J. Am. Chem. Soc.* **1996**, *118*, 2117−2125.
(42) Allard, J.; Grochulski, P.; Sygusch, J. Covalent Intermediate Trapped in 2-Keto-3-Deoxy-6-Phosphogluconate (KDPG) Aldolase Structure at 1.95-Angstrom Resolution. *Proc. Natl. Acad. Sci. U.S.A.* **2001**, *98*, 3679−3684.
(43) Noy, A.; Vezenov, D. V.; Lieber, C. M. Chemical Force Microscopy. *Annu. Rev. Mater. Sci.* **1997**, *27*, 381−421.
(44) Moy, V. T.; Florin, E. L.; Gaub, H. E. Adhesive Forces between Ligand and Receptor Measured by AFM. *Colloids Surf., A* **1994**, *93*, 343−348.
(45) Morris, V. J.; Gromer, A.; Kirby, A. R.; Bongaerts, R. J. M.; Gunning, A. P. Using AFM and Force Spectroscopy to Determine Pectin Structure and (Bio) Functionality. *Food Hydrocolloids* **2011**, *25*, 230−237.